AGU PUBLICATIONS

Geophysical Research Letters

RESEARCH LETTER
10.1002/2016GL068691

Key Points:
- First observation of a tripolar guide field perturbation at Earth's magnetopause
- Observation is consistent with asymmetric Hall magnetic fields between two X lines
- Symmetric-like magnetopause conditions and a guide field are likely required for its development

Correspondence to:
S. Eriksson,
eriksson@lasp.colorado.edu

Citation:
Eriksson, S., P. A. Cassak, A. Retinò, and F. S. Mozer (2016), Subsolar magnetopause observation and kinetic simulation of a tripolar guide magnetic field perturbation consistent with a magnetic island, *Geophys. Res. Lett., 43*, 3035–3041, doi:10.1002/2016GL068691.

Received 14 MAR 2016
Accepted 20 MAR 2016
Accepted article online 25 MAR 2016
Published online 6 APR 2016

Subsolar magnetopause observation and kinetic simulation of a tripolar guide magnetic field perturbation consistent with a magnetic island

S. Eriksson[1], P. A. Cassak[2], A. Retinò[3], and F. S. Mozer[4]

[1]Laboratory for Atmospheric and Space Physics, University of Colorado Boulder, Boulder, Colorado, USA, [2]Department of Physics and Astronomy, West Virginia University, Morgantown, West Virginia, USA, [3]Laboratoire de Physique des Plasmas, École Polytechnique, Paris, France, [4]Space Sciences Laboratory, University of California, Berkeley, California, USA

Abstract The Polar satellite recorded two reconnection exhausts within 6 min on 1 April 2001 across a subsolar magnetopause that displayed a symmetric plasma density, but different out-of-plane magnetic field signatures for similar solar wind conditions. The first magnetopause crossing displayed a bipolar guide field variation in a weak external guide field consistent with a symmetric Hall field from a single X line. The subsequent crossing represents the first observation of a tripolar guide field perturbation at Earth's magnetopause in a strong guide field. This perturbation consists of a significant guide field enhancement between two narrow guide field depressions. A particle-in-cell simulation for the prevailing conditions across this second event resulted in a magnetic island between two simulated X lines across which a tripolar guide field developed consistent with the observation. The simulated island supports a scenario whereby Polar encountered the asymmetric quadrupole Hall magnetic fields between two X lines for symmetric conditions across the magnetopause.

1. Introduction

Whether magnetic field reconnection [e.g., *Priest and Forbes*, 2000] proceeds via a dominant single X line or to some extent via multiple competing X lines [e.g., *Nishida*, 1989] at the Earth's dayside magnetopause is a topic of great importance for our understanding of the structure and dynamics of this boundary that ultimately allows for a transport of plasma, momentum, and energy between the upstream solar wind and the Earth's magnetosphere.

A multiple X line scenario has been proposed as one of several mechanisms for the generation of magnetic flux ropes and "flux transfer events" at the dayside magnetopause [e.g., *Lee and Fu*, 1985; *Raeder*, 2006; *Hasegawa et al*., 2010, 2015; *Sibeck and Lin*, 2011; *Øieroset et al*., 2011], while a patchy, single X line scenario was proposed by *Russell and Elphic* [1978]. A northward moving flux rope on the dayside magnetopause during southward interplanetary magnetic field (IMF) will result in a bipolar perturbation of the normal component of the magnetic field (B_N) with an outward $B_N > 0$ followed by an earthward $B_N < 0$. However, flux ropes forming in the subsolar region may be stagnant for some initial period of growth or move at a substantially lower speed in the north-south direction relative to the normal motion of the magnetopause such that a bipolar B_N may be weak or absent as observed by a satellite across the equatorial magnetopause.

Evidence for reconnection across a current sheet involves several characteristic signatures such as two oppositely accelerated jets of plasma from an X line [e.g., *Paschmann et al*., 1986; *Sonnerup et al*., 1981] and a Hall field perturbation of the out-of-plane component of the magnetic field [e.g., *Sonnerup*, 1979; *Terasawa*, 1983]. This Hall field depends on the magnitude of the external guide field [e.g., *Karimabadi et al*., 1999] and the relative magnitude of the plasma density on either side of the current sheet [e.g., *Birn et al*., 2008; *Mozer et al*., 2008; *Malakit et al*., 2010].

In the basic case with no external guide field, a symmetric plasma density, and a symmetric magnetic field strength across the current sheet, the Hall magnetic field consists of a symmetric quadrupole field [e.g., *Birn et al*., 2001] with two lobes of positive guide field and two lobes of negative guide field. This results in a bipolar variation of the out-of-plane magnetic field across each of the two exhausts as reported in the magnetotail [e.g., *Øieroset et al*., 2001] and across a subsolar magnetopause for symmetric conditions [*Mozer et al*., 2002]. A positive external guide magnetic field expands the regions of the two positive lobes

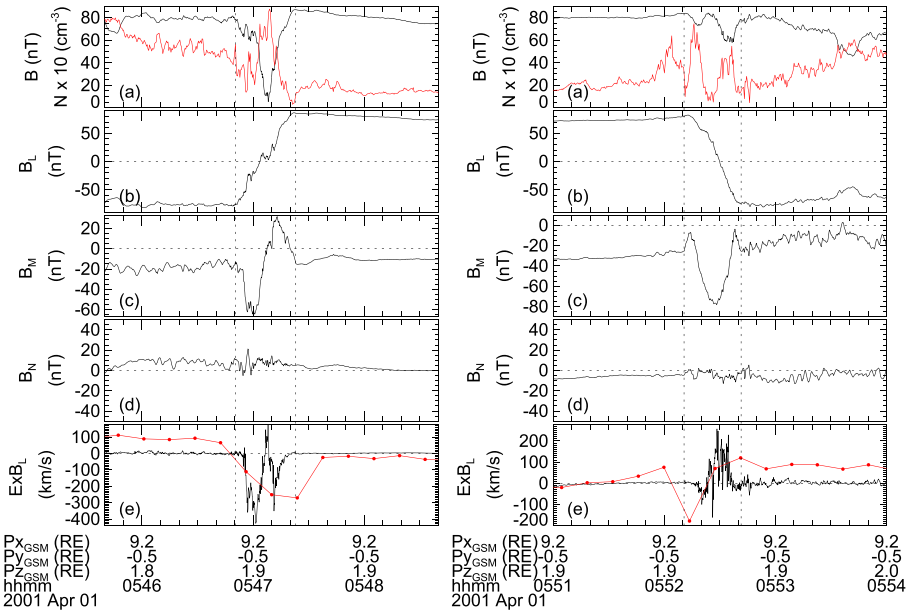

Figure 1. Polar observations are shown in boundary normal LMN coordinates across two dayside magnetopause crossings on 1 April 2001 with very different signatures of the out-of-plane (B_M) magnetic field with a bipolar B_M at 0547:10 UT and a tripolar B_M at 0552:30 UT. The panels display (a) magnetic field strength (black) and a plasma number density (multiplied by a factor of 10) derived from the spacecraft potential (red), (b) antiparallel B_L component, (c) guide field B_M component, (d) normal B_N component of the magnetic field, and (e) the exhaust L components of the ion plasma velocity (red) and the $\mathbf{E}\times\mathbf{B}$ drift (black). The locally obtained LMN directions from minimum variance analyses are $\mathbf{L}_{GSM}=(-0.236, -0.109, 0.966)$, $\mathbf{M}_{GSM}=(-0.048, -0.991, -0.124)$, and $\mathbf{N}_{GSM}=(0.971, -0.076, 0.229)$ at 0547:10 UT, and $\mathbf{L}_{GSM}=(-0.190, -0.374, 0.908)$, $\mathbf{M}_{GSM}=(0.059, -0.927, -0.370)$, and $\mathbf{N}_{GSM}=(0.980, -0.017, 0.198)$ at 0552:30 UT.

at the expense of the two negative lobes [e.g., *Ma et al.*, 1994; *Karimabadi et al.*, 1999; *Eastwood et al.*, 2010] or vice versa in the case of a negative guide field.

Here we report the first known observation of a tripolar guide field perturbation signature across a symmetric dayside magnetopause in the presence of an external guide field, reminiscent of recent solar wind observations [*Eriksson et al.*, 2014, 2015]. We compare this subsolar observation by the Polar satellite with the results of a kinetic simulation of magnetic reconnection. The comparison supports a scenario whereby the observed tripolar perturbation is consistent with an oblique satellite trajectory across the asymmetric quadrupole Hall magnetic fields from two X lines and the presence of a magnetic island between them.

2. Polar Observations at the Subsolar Magnetopause

Figure 1 compares observations from two magnetopause crossings in the subsolar region as recorded at 0547:10 UT and 0552:30 UT on 1 April 2001 by the Polar satellite [*Harvey et al.*, 1995; *Russell et al.*, 1995; *Scudder et al.*, 1995]. The Polar data are displayed in a boundary normal LMN coordinate system using a minimum variance analysis of the local magnetic fields [*Sonnerup and Scheible*, 1998]. The unit vectors employed for the first event are $\mathbf{L}=(-0.236, -0.109, 0.966)$, $\mathbf{M}=(-0.048, -0.991, -0.124)$, and $\mathbf{N}=(0.971, -0.076, 0.229)$ in GSM coordinates. The original **L** and **M** vectors were rotated by −12° about this **N** axis such that the guide magnetic field is displayed with an equal $B_M=-14$ nT on the two sides of the magnetopause. Minimum variance analysis across the second event resulted in a similar set of unit vectors $\mathbf{L}=(-0.190, -0.374, 0.908)$, $\mathbf{M}=(0.059, -0.927, -0.370)$, and $\mathbf{N}=(0.980, -0.017, 0.198)$. Note that the out-of-plane **M** directions point mostly along the negative Y_{GSM} direction.

The first inbound magnetopause crossing displays a bipolar B_M guide field perturbation across a southward reconnection exhaust rather than just a negative and unipolar B_M perturbation, which would have been expected for a strong plasma density gradient at the magnetopause [e.g., *Mozer et al.*, 2008; *Malakit et al.*, 2010]. This bipolar B_M event was first reported by *Mozer et al.* [2002]. It displays a positive $B_N>0$ normal field

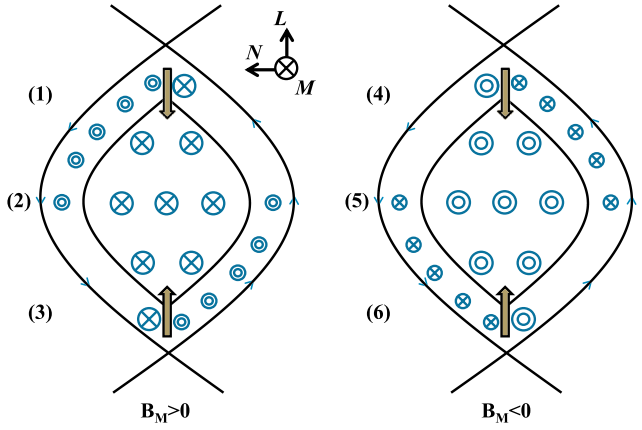

Figure 2. Schematic of the out-of-plane magnetic field (blue symbols) in a magnetic island between two active X lines for symmetric conditions and a finite guide field $B_M > 0$ (left) and $B_M < 0$ (right). Black solid lines with blue arrows indicate the direction of the in-plane magnetic field. The magnetosheath ($B_L < 0$) is on the left side of both scenarios. Bold vertical arrows indicate the exhaust directions. Numbers mark regions of expected bipolar (1, 3, 4, and 6) and tripolar (2 and 5) field perturbations for satellite trajectories along the normal **N** direction through stationary islands while oblique trajectories are expected for drifting islands.

and a negative B_M deflection toward the magnetosheath side ($B_L < 0$) and a positive B_M deflection toward the magnetospheric side ($B_L > 0$) consistent with the southern section of a quadrupole Hall magnetic field centered at a single X line to the north of the Polar satellite. A quadrupole Hall field is in agreement with the observed weak guide field ratio $B_M/B_L = 0.18$ and the rather symmetric plasma density conditions that Polar recorded on either side of the magnetopause at this time with $N \sim 5\,\mathrm{cm}^{-3}$ in the adjacent magnetosheath and $N \sim 2\,\mathrm{cm}^{-3}$ on the earthward side of the magnetopause.

The subsequent outbound crossing (Figure 1, right column) occurred less than 6 min later at which time Polar recorded an intriguing tripolar B_M guide field perturbation for a stronger $B_M/B_L = 0.33$ guide field ratio. This tripolar signature which is reminiscent of solar wind observations by Cluster [*Eriksson et al*., 2015] displayed two B_M depressions on either side of an enhanced B_M at the center of a current sheet with a B_L rotation from 80 nT on the magnetosphere side to −73 nT on the magnetosheath side. Significant density variations, likely related to pressure balance, were also observed around this tripolar event including a deep density minimum within the central period of the enhanced guide magnetic field. This second event was characterized by an earthward $B_N < 0$ normal field, and there was a strong northward 200 km/s $\mathbf{E} \times \mathbf{B}$ exhaust flow observed toward the magnetosheath side ($B_L < 0$) of the current sheet consistent with an X line to the south of the Polar satellite. In a highly symmetric situation like this, with $N = 2.2\,\mathrm{cm}^{-3}$ on the magnetosphere side and $N = 2.0\,\mathrm{cm}^{-3}$ on the adjacent magnetosheath side of the current sheet, we would expect a bipolar B_M perturbation of a quadrupole Hall field to consist of a positive B_M deflection toward the magnetosheath side ($B_L < 0$) and a negative B_M deflection toward the magnetospheric side ($B_L > 0$). However, Polar clearly observed an additional positive B_M deflection at the innermost, earthward edge of the current sheet. This perturbation would be consistent with a Hall magnetic field if an X line was also present to the north of the satellite. The lower resolution ion velocity measurement from the plasma instrument indeed suggests that Polar encountered a southward 200 km/s V_L deflection at 0552:14 UT toward the side dominated by a $B_L > 0$ at the time of this additional positive B_M deflection which is in agreement with a northern X line.

The ion velocity observation is composed of a perpendicular and a parallel component relative to the magnetic field while the $\mathbf{E} \times \mathbf{B}$ measurement, of course, does not capture a parallel component of the ion velocity. This may explain the apparent deviations between these measurements of the L components of the ion flow on either side of the magnetopause. A more significant parallel ion flow may have been present in the adjacent magnetosheath, and also at the time of the enhanced negative V_L observation, since the magnetic field was dominated by the B_L component during both of these intervals. Finally, it appears that the low-resolution V_L measurement did not completely capture the interval of the more localized and positive $(\mathbf{E} \times \mathbf{B})_L$ jet.

In summary, we propose that Polar traversed a magnetic island in the subsolar magnetopause region at 0552:30 UT between a northern X line ($V_L < 0$ jet and a $B_M > 0$ deflection toward $B_L > 0$) and a southern X line ($(\mathbf{E} \times \mathbf{B})_L > 0$ flow and a $B_M > 0$ deflection toward $B_L < 0$) as illustrated on the right-hand side of the Figure 2 schematic. It is likely that the Polar satellite was closer to the southern X line since the normal magnetic field was dominated by an earthward $B_N < 0$. In this scenario with a background negative guide field and a dominant $B_M < 0$ in the center of the island, the two positive $B_M > 0$ deflections of the tripolar perturbation

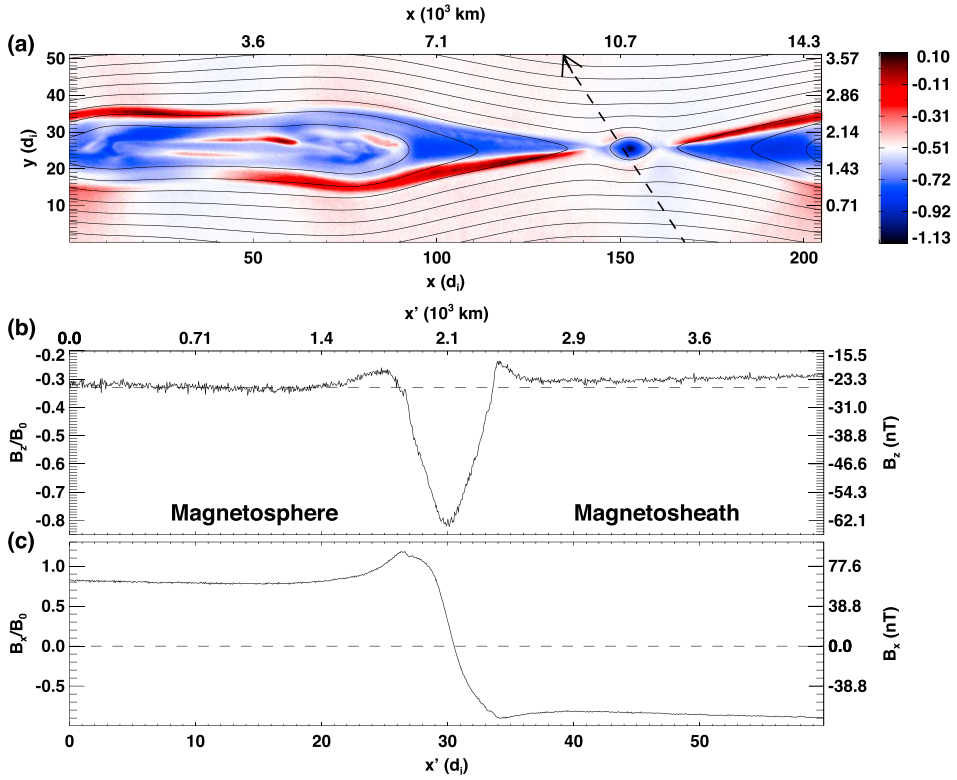

Figure 3. (a) Simulated out-of-plane magnetic field (color) and in-plane field lines (black) for nearly symmetric conditions. An oblique arrowed line indicates a virtual spacecraft trajectory from the magnetosphere (bottom half) to the magnetosheath (top half); (b) out-of-plane (B_z) field component along the indicated trajectory with the along-track distance shown along the x' axis; (c) reconnecting (B_x) field component along the x' axis. Normalized units are shown on the lower and left axes of each panel with physical units shown on the top and right axes. A tripolar guide field perturbation is seen with two field depressions on either side of a magnetic island with a strong core field.

correspond to individual lobes of two asymmetric quadrupole Hall magnetic fields originating from two X lines. The sense of these narrow deflections will change from positive to negative if the background guide field instead is positive as illustrated on the left of the Figure 2 schematic.

3. PIC Simulation Results of Dayside Symmetric Reconnection With a Guide Field

We now explore the numerical results from an electromagnetic particle-in-cell (PIC) simulation of reconnection using the *P3D* code [*Zeiler et al.*, 2002; *Drake et al.*, 2006] in order to better understand the observed tripolar guide field perturbation at the magnetopause. This code advances particles using a relativistic Boris stepper with electromagnetic fields extrapolated to the particles' positions [*Birdsall and Langdon*, 2004]. Electromagnetic fields are evolved using the trapezoidal leapfrog method on Maxwell's equations with second-order spatial derivatives, while using a smaller time step to resolve light waves. The electrostatic electric field is corrected by solving Poisson's equation to ensure charge conservation.

Figure 3 shows the simulated out-of-plane magnetic field for parameters chosen to be similar to those observed by the Polar satellite during the tripolar event in Figure 1. The two-dimensional simulation employed periodic boundary conditions and two oppositely directed current sheets with an initial thickness of one ion skin depth (1 $d_i = c/\omega_{pi}$) on a 204.8 × 102.4 numerical grid with a grid scale of 0.05 in units of c/ω_{pi} in each direction and 500 particles per grid cell. Here c/ω_{pi} is based on a chosen normalized density $N_0 = 10.2\ \mathrm{cm}^{-3}$. The mass ratio m_i/m_e of ions to electrons was 25, and the speed of light was 15 times the normalized Alfvén speed ($\omega_{pi}/\Omega_{ci} = 15$). The simulation used upstream (asymptotic) field and plasma parameters in normalized units ($B_0 = B_{L2} = 77.6$ nT and $N_0 = 10.2\ \mathrm{cm}^{-3}$) of $B_{L1} = 0.95$, $B_{L2} = 1.00$, $N_1 = 0.25$, $N_2 = 0.20$, $T_{e1} = 0.330$, $T_{e2} = 0.481$, $T_{i1} = 0.658$, and $T_{i2} = 0.50$ with a uniform guide field $B_M = 0.33$. Subscript "1" corresponds to the magnetosphere (bottom half), and subscript "2" corresponds to the magnetosheath (top half).

It is noted that the magnetic fields and plasma number densities were chosen to be close to the measured values. The ion and electron temperatures were constrained such that the simulated magnetopause current sheet satisfied pressure balance.

The simulation produced a tripolar guide field perturbation along an oblique trajectory through a magnetic island at time $t = 100$ that formed 3.3 s prior to the time of the cut displayed in Figure 3. This out-of-plane field signature is qualitatively consistent with the Polar observations and the Figure 2 schematic. Each of the two X lines supports an asymmetric quadrupole Hall magnetic field consisting of two wide lobes of negative (blue) field deflections and two narrow lobes of positive (red) field deflections. This asymmetry is consistent with a negative background guide field [e.g., *Karimabadi et al*., 1999]. Polar observed a maximum core field of $B_M = -51$ nT which was twice as strong as the external guide fields of -26 nT and -25 nT on the two sides. This compares very well with the simulated core field of the island which was 2.47 times stronger than the guide field. Finally, Polar observed maximum guide field depressions of 18 nT and 19 nT on the two sides of the core field region. This corresponds to 71% and 75% of the adjacent guide field magnitudes on the magnetospheric and magnetosheath sides of the two dips. The simulation resulted in somewhat weaker depressions at 20% and 29% relative to the adjacent guide field magnitude. It is not clear why the observed and simulated depressions differ in magnitude, although several factors such as time evolution and three-dimensional effects may play an important role.

4. Discussion

The magnetopause is typically considered as an asymmetric boundary between a very low plasma density and a strong magnetic field on the earthward side, and a high plasma density and relatively weaker magnetic field in the adjacent magnetosheath. These conditions are expected to result in a distorted Hall magnetic field that consists of one unipolar and negative Hall field perturbation ($\Delta B_M < 0$) to the south of the X line and one unipolar and positive Hall field perturbation ($\Delta B_M > 0$) to the north of the X line [e.g., *Mozer et al*., 2008; *Malakit et al*., 2010].

Symmetric plasma density and magnetic field conditions may develop across the dayside subsolar magnetopause depending on the upstream solar wind conditions. This is especially likely during a formation of a plasma depletion layer (PDL) [e.g., *Anderson and Fuselier*, 1993; *Anderson et al*., 1997] in the magnetosheath just upstream of the magnetopause. Its presence may be explained as due to an imbalance between the rates of magnetic reconnection at the dayside magnetopause, which removes magnetic flux and prevents the field from building up in the subsolar region, and the rate at which solar wind magnetic flux is added continuously to this magnetosheath region. An imbalance of these rates with a higher influx of solar wind magnetic fields will compress the draped magnetosheath magnetic field against the magnetopause and force plasma away from this region along the magnetic field. The result is a PDL with compressed magnetic field and decreased plasma density. A PDL is more likely during northward IMF conditions [e.g., *Wang et al*., 2003]. However, it may also form during southward IMF conditions when the upstream solar wind dynamic pressure is high as discussed by *Anderson et al*. [1997].

Figure 4 compares the upstream solar wind observations from ACE with Polar observations in the magnetosheath. The ACE data were shifted forward in time by ~29 min to maximize the correlation of the measured IMF clock angles at ACE and Polar. The solar wind density was also multiplied by a factor of 4 to estimate an average magnetosheath density of 9.6 cm^{-3} and 8.4 cm^{-3} at the time of the two magnetopause crossings by the Polar satellite. These times are indicated between the two pairs of vertical dashed lines in Figure 4. The upstream conditions were characterized by a very fast earthward solar wind stream at ~815 km/s and an IMF magnitude of about 8 nT. Polar generally observed a lower plasma density in the magnetosheath throughout the 1 h period shown in Figure 4 as compared with the estimated shocked plasma density from ACE. This relatively lower density and the fast, steady solar wind speed indicate a possible PDL formation despite the presence of a strong southward IMF $B_z = -6.3$ nT at the time of both magnetopause crossings [*Anderson et al*., 1997]. The most pronounced change of the solar wind between the two Polar observations was related to a strengthening of the IMF B_y from 3.7 nT during the first inbound crossing to 5.3 nT at the time of the subsequent outbound event. A 43% stronger upstream IMF B_y is consistent with a stronger external guide field as observed by Polar during the intriguing tripolar event that likely contributed to the strong core magnetic field observed at the center of this perturbation signature.

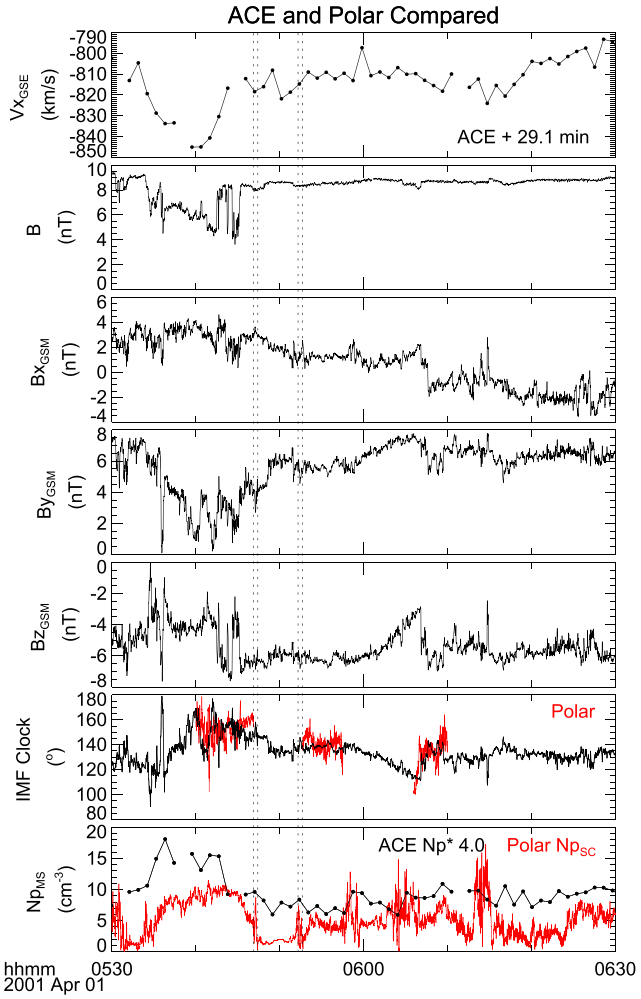

Figure 4. Solar wind observations from the upstream ACE satellite (black color) compared with Polar satellite observations (red color). Panels from the top show the V_x component of the solar wind velocity; the magnitude of the interplanetary magnetic field (IMF); B_x, B_y, and B_z components of the IMF in GSM coordinates; IMF clock angle $\theta = \arctan(B_y/B_z)$; and the plasma number density from ACE (multiplied by a factor of 4) and Polar based on the spacecraft potential. The two pairs of vertical dashed lines mark the times of the two Polar magnetopause events discussed in this letter.

The tripolar signature was observed to last ~31 s along the Polar trajectory across the magnetopause. This duration may be used together with a deHoffmann-Teller velocity $\mathbf{V}_{HT} = (V_{HTL}, V_{HTM}, V_{HTN}) = (71, -9, -73)$ km/s [*Khrabrov and Sonnerup*, 1998] at 0551–0554 UT to estimate an along-track spatial dimension (d) of the event. The northward V_{HTL} and earthward V_{HTN} motion of the magnetopause is consistent with a northward moving structure with an in-plane NL dimension $d = 3158$ km or $20.3d_i$ along the Polar satellite trajectory and an estimated normal width of ~2250 km or $14.5d_i$. Here $d_i = 156$ km is the average ion skin depth ($d_i = c/\omega_{pi}$ and $\omega_{pi} = (N_0e^2/m_p\varepsilon_0)^{1/2}$) based on plasma number densities $N = 2.2\,\mathrm{cm}^{-3}$ on the magnetospheric side and $N = 2.0\,\mathrm{cm}^{-3}$ in the adjacent magnetosheath. This estimated 3158 km along-track width of the observed tripolar signature is approximately 3–4 times as wide as compared with a simulated width of 720–1120 km across a few oblique cuts of the simulated magnetic island at time $t = 100$.

5. Conclusions

We have reported the first observed tripolar guide field perturbation at Earth's dayside magnetopause as observed by the Polar satellite at 0552:30 UT across a subsolar region on 1 April 2001. The signature consisted of a significant strengthening of the background guide field at the current sheet and two adjacent guide field depressions with $\Delta B_M/B_M = 71$–75%. Similar tripolar signatures have been observed across exhausts in the solar wind [*Eriksson et al.*, 2014, 2015] where symmetric plasma and field conditions tend to be present. However, this is the first time that this type of signature is observed along the direction of the guide magnetic field at the Earth's dayside magnetopause for relatively unusual conditions of symmetric magnitudes of plasma density and magnetic field.

A PIC simulation of reconnection for the observed guide field ratio $B_M/B_L = 0.33$ and symmetric conditions reproduced a very similar tripolar field across a magnetic island that formed between two X lines. The estimated dimension of the observed tripolar field and the simulated size of the magnetic island are comparable. The observed and simulated out-of-plane magnetic fields both showed a significant strengthening of the negative guide field which formed a negative core field that was twice as strong as the external guide field. This core field was sandwiched between two narrow lobes of depressed guide field. The Polar data and PIC simulations support a scenario whereby the observed tripolar field is consistent with an oblique trajectory through a magnetic island between two active X lines and the asymmetric quadrupole Hall magnetic field expected at each X line for symmetric conditions and a finite guide field. A tripolar guide field

perturbation may therefore be used as evidence for the presence of two X lines and a magnetic island across symmetric current sheets.

Acknowledgments
This research is supported by NASA grants NNX08AO84G, NNX12AH43G, and NNX16AF75G to the University of Colorado at Boulder (S.E.) and NSF grants AGS-0953463 and AGS-1460037 to the West Virginia University (P.A.C.). Polar observations are available via the NASA CDAWeb and upon request from S.E. and A.R. The simulation data used to produce the results of this paper are available from P.A.C. S.E. and P.A.C. acknowledge the hospitality of NORDITA, Stockholm, Sweden, at which some of the work was discussed and finalized.

References

Anderson, B. J., and S. A. Fuselier (1993), Magnetic pulsations from 0.1 to 4.0 Hz and associated plasma properties in the Earth's subsolar magnetosheath and plasma depletion layer, *J. Geophys. Res.*, *98*, 1461–1479, doi:10.1029/92JA02197.

Anderson, B. J., T. D. Phan, and S. A. Fuselier (1997), Relationships between plasma depletion and subsolar reconnection, *J. Geophys. Res.*, *102*, 9531–9542, doi:10.1029/97JA00173.

Birdsall, C. K., and A. B. Langdon (2004), *Plasma Physics Via Computer Simulation*, Taylor and Francis.

Birn, J., et al. (2001), Geospace Environmental Modeling (GEM) magnetic reconnection challenge, *J. Geophys. Res.*, *106*, 3715–3719, doi:10.1029/1999JA900449.

Birn, J., J. E. Borovsky, and M. Hesse (2008), Properties of asymmetric magnetic reconnection, *Phys. Plasmas*, *15*, 032101-1, doi:10.1063/1.2888491.

Drake, J. F., M. Swisdak, K. M. Schoeffler, B. N. Rogers, and S. Kobayashi (2006), Formation of secondary islands during magnetic reconnection, *Geophys. Res. Lett.*, *33*, L13105, doi:10.1029/2006GL025957.

Eastwood, J. P., M. A. Shay, T. D. Phan, and M. Øieroset (2010), Asymmetry of the ion diffusion region Hall electric and magnetic fields during guide field reconnection: Observations and comparison with simulations, *Phys. Rev. Lett.*, *104*, doi:10.1103/PhysRevLett.104.205001.

Eriksson, S., D. L. Newman, G. Lapenta, and V. Angelopoulos (2014), On the signatures of magnetic islands and multiple X-lines in the solar wind as observed by ARTEMIS and WIND, *Plasma Phys. Controlled Fusion*, *56*, 064008.

Eriksson, S., G. Lapenta, D. L. Newman, T. D. Phan, J. T. Gosling, B. Lavraud, Y. V. Khotyaintsev, C. M. Carr, S. Markidis, and M. V. Goldman (2015), On multiple reconnection X-lines and tripolar perturbations of strong guide magnetic fields, *Astrophys. J.*, *805*, 43, doi:10.1088/0004-637X/805/1/43.

Harvey, P., et al. (1995), The electric field instrument on the Polar satellite, *Space Sci. Rev.*, *71*, 583–596.

Hasegawa, H., et al. (2010), Evidence for a flux transfer event generated by multiple X-line reconnection at the magnetopause, *Geophys. Res. Lett.*, *37*, L16101, doi:10.1029/2010GL044219.

Hasegawa, H., B. U. O. Sonnerup, S. Eriksson, T. K. M. Nakamura, and H. Kawano (2015), Dual-spacecraft reconstruction of a three-dimensional magnetic flux rope at the Earth's magnetopause, *Ann. Geophys.*, *33*, 169, doi:10.5194/angeo-33-169-2015.

Karimabadi, H., D. Krauss-Varban, N. Omidi, and H. X. Vu (1999), Magnetic structure of the reconnection layer and core field generation in plasmoids, *J. Geophys. Res.*, *104*, 12,313–12,326, doi:10.1029/1999JA900089.

Khrabrov, A. V., and B. U. Ö. Sonnerup (1998), DeHoffmann-Teller analysis, in *Analysis Methods for Multi-Spacecraft Data*, edited by G. Paschmann and P. W. Daly, *ISSI Sci. Rep. SR-001*, pp. 221–248, Eur. Space Agency Publ. Div., Noordwijk, Netherlands.

Lee, L.-C., and Z.-F. Fu (1985), A theory of magnetic flux transfer at the Earth's magnetopause, *Geophys. Res. Lett.*, *12*, 105–108, doi:10.1029/GL012i002p00105.

Ma, Z. W., A. Otto, and L. C. Lee (1994), Core magnetic field enhancement in single X line, multiple X line and patchy reconnection, *J. Geophys. Res.*, *99*, 6125–6136, doi:10.1029/93JA03480.

Malakit, K., M. A. Shay, P. A. Cassak, and C. Bard (2010), Scaling of asymmetric magnetic reconnection: Kinetic particle-in-cell simulations, *J. Geophys. Res.*, *115*, A10223, doi:10.1029/2010JA015452.

Mozer, F. S., S. D. Bale, and T. D. Phan (2002), Evidence of diffusion regions at a subsolar magnetopause crossing, *Phys. Rev. Lett.*, *89*, 015002-1, doi:10.1103/PhysRevLett.89.015002.

Mozer, F. S., V. Angelopoulos, J. Bonnell, K.-H. Glassmeier, and J. P. McFadden (2008), THEMIS observations of modified Hall fields in asymmetric magnetic field reconnection, *Geophys. Res. Lett.*, *35*, L17S04, doi:10.1029/2007GL033033.

Nishida, A. (1989), Can random reconnection on the magnetopause produce the low-latitude boundary layer?, *Geophys. Res. Lett.*, *16*, 227–230, doi:10.1029/GL016i003p00227.

Øieroset, M., T. D. Phan, M. Fujimoto, R. P. Lin, and R. P. Lepping (2001), In-situ detection of collisionless reconnection in the Earth's magnetotail, *Nature*, *412*, 414–416.

Øieroset, M., T. D. Phan, J. P. Eastwood, M. Fujimoto, W. Daughton, M. A. Shay, V. Angelopoulos, F. S. Mozer, J. P. McFadden, D. E. Larson, and K.-H. Glassmeier (2011), Direct evidence for a three-dimensional magnetic flux rope flanked by two active magnetic reconnection X lines at Earth's magnetopause, *Phys. Rev. Lett.*, *107*, 165007.

Paschmann, G., I. Papamastorakis, W. Baumjohann, N. Sckopke, C. W. Carlson, B. U. Ö. Sonnerup, and H. Luhr (1986), The magnetopause for large magnetic shear: AMPTE/IRM observations, *J. Geophys. Res.*, *91*, 11,099–11,119, doi:10.1029/JA091iA10p11099.

Priest, E., and T. Forbes (2000), *Magnetic Reconnection: MHD Theory and Applications*, Cambridge Univ. Press, New York.

Raeder, J. (2006), Flux Transfer Events: 1. Generation mechanism for strong southward IMF, *Ann. Geophys.*, *24*, 381, doi:10.5194/angeo-24-381-2006.

Russell, C. T., and R. C. Elphic (1978), Initial ISEE magnetometer results: Magnetopause observations, *Space Sci. Rev.*, *22*, 681.

Russell, C. T., R. C. Snare, J. D. Means, D. Pierce, D. Dearborn, M. Larson, G. Barr, and G. Le (1995), The GGS/Polar magnetic fields investigation, *Space Sci. Rev.*, *71*, 563–582.

Scudder, J., et al. (1995), HYDRA—A 3-dimensional electron and ion hot plasma instrument for the Polar spacecraft of the GGS mission, *Space Sci. Rev.*, *71*, 459–495.

Sibeck, D. G., and R.-Q. Lin (2011), Concerning the motion and orientation of flux transfer events produced by component and antiparallel reconnection, *J. Geophys. Res.*, *116*, A07206, doi:10.1029/2011JA016560.

Sonnerup, B. U. Ö. (1979), Magnetic field reconnection, in *Solar System Plasma Physics*, edited by L. J. Lanzerotti, C. Kennel, and E. Parker, pp. 47–108, North-Holland, Amsterdam.

Sonnerup, B. U. Ö., and M. Scheible (1998), Minimum and maximum variance analysis, in *Analysis Methods for Multi-Spacecraft Data*, edited by G. Paschmann and P. W. Daly, *ISSI Sci. Rep. SR-001*, pp. 185–220, Eur. Space Agency Publ. Div., Noordwijk, Netherlands.

Sonnerup, B. U. Ö., G. Paschmann, I. Papamastorakis, N. Sckopke, G. Haerendel, S. J. Bame, J. R. Asbridge, J. T. Gosling, and C. T. Russell (1981), Evidence for magnetic field reconnection at the Earth's magnetopause, *J. Geophys. Res.*, *86*, 10,049–10,067, doi:10.1029/JA086iA12p10049.

Terasawa, T. (1983), Hall current effect on tearing mode instability, *Geophys. Res. Lett.*, *10*, 475–478, doi:10.1029/GL010i006p00475.

Wang, Y. L., J. Raeder, C. T. Russell, T. D. Phan, and M. Manapat (2003), Plasma depletion layer: Event studies with a global model, *J. Geophys. Res.*, *108*(A1), 1010, doi:10.1029/2002JA009281.

Zeiler, A., D. Biskamp, J. F. Drake, B. N. Rogers, M. A. Shay, and M. Scholer (2002), Three-dimensional particle simulations of collisionless magnetic reconnection, *J. Geophys. Res.*, *107*(A9), 1230, doi:10.1029/2001JA000287.